

Automatic calculation of two-loop ELWK corrections to the muon ($g-2$)^{*}

Tadashi Ishikawa¹, Nobuya Nakazawa² and Yoshiaki Yasui³

¹ High Energy Accelerator Organization(KEK), 1-1 OHO Tsukuba Ibaraki 305-0801,Japan

² Department of Physics, Kogakuin University, Shinjuku, Tokyo 163-8677, Japan

³ Department of Management, Tokyo Management College, Ichikawa, Chiba 272-0001, Japan

E-mail: nobuya@suchix.kek.jp

Abstract. Two-loop electroweak corrections to the muon anomalous magnetic moment are automatically calculated by using GRACE-FORM system, as a trial to extend our system for two-loop calculation. We adopt the non-linear gauge (NLG) to check the reliability of our calculation. In total 1780 two-loop diagrams consisting of 14 different topological types and 70 one-loop diagrams composed of counter terms are calculated. We check UV- and IR-divergences cancellation and the independence of the results from NLG parameters. As for the numerical calculation, we adopt trapezoidal rule with Double Exponential method (DE). Linear extrapolation method (LE) is introduced to regularize UV- and IR- divergences and to get finite values.

1. Introduction

In order to get a sign of beyond the standard model physics from high precision experimental data, we need higher order radiative corrections within Standard Model (SM). For this purpose our group has been developing the automatic calculation system GRACE [1] since the late 1980's. The measurement of the muon anomalous magnetic moment ($g-2$) is the one of the most precise experiments to check the SM. QED correction was calculated by T.Kinoshita et al. [2] up to tenth-order. The two-loop electroweak (ELWK) correction to ($g-2$) was calculated approximately by Kukhto et al. [3] in 1992. Surprisingly, the two-loop correction is almost 20% of the one-loop correction. We started to calculate the full two-loop corrections in 1995 and presented our formalism at Pisa conference [4]. We also showed that the two-loop QED value [5] was correctly reproduced within our general formalism. However, the number of diagrams is huge (1780+70) and the numerical integration requires the big CPU-power to achieve required accuracy, we must wait until various environments are improved.

During these days, the several groups did the calculations using leading $\log(M^2)$ approximations. (M =heavy particle mass) [6] [7] and the approximate value of the two-loop ELWK correction is widely accepted [8]. In 2001, BNL-Experiment 821 [9] announced that the precise experimental value deviates from that of SM around $(2.2 \sim 2.7) \sigma$. It brought much interest in the theoretical value.

^{*}To appear in the proceedings of the 4th Computational Particle Physics Workshop, October 2016, Hayama, Japan.

The various theoretical predictions and experimental value are summarized in the next subsection. The main theoretical concern is shifted to the hadronic contributions.

1.1. present status of the theoretical predictions of $(g-2)$ and future experiments

We summarize the present theoretical predictions of muon $(g-2)$ in Table 1.

Table 1: Theoretical predictions of muon $(g-2)$ [10]

Type of correction	Numerical Value (unit 10^{-11})	Error	Reference
QED up to tenth-order	116584718.95	(0.08)	[2]
Leading Order Hadronic Vac.Pol.	6923	(42)(3)	[11]
NLO Vac.Pol.+Hadronic LBL	7	(26)	[12]
ELWK (one-loop)	195.82	(0.02)	[13]
ELWK (two-loop)	- 41.2	(1.0)	[3][6][7][14]
Theory total	116591803	(1)(42)(26)	[10]
Experimental Value	116592091	(54)(33)	[9][15]

The discrepancy between the experimental value and the theoretical value is still large. As new experiments are scheduled at FNAL-E989 [16] and J-PARC-E034 [17], we can expect to have new data within a few years.

1.2. Purpose of our calculation

Although the two-loop ELWK correction is almost established as summarized in the Table 1, we try to get the value without any approximation to confirm the validity of the earlier studies. It is also an important trial to extend GRACE-system from one-loop to two-loop calculation. It may become a milestone to construct the framework of Perturbative Numerical Quantum Field Theory (PNQFT). The concepts of PNQFT are summarized as follows. (a) It is essential to assume amplitudes as meromorphic functions of space time dimension n , for extracting both UV- and IR-divergences. By adopting dimensional regularization, gauge invariant renormalized value is obtained directly. (b) The source for numerical integration is automatically generated by a symbolic manipulation system. (c) It is crucial to reduce human intervention to avoid careless mistakes, so that numerical method is fully exploited. The following calculation shows the outline of this direction.

In section 2 and 3, we briefly explain the flow and foundation of our calculation. In section 4, we touch on our method of numerical calculation. We emphasize that the Linear Extrapolation (LE) method [18] is simple and efficient method to regularize UV- and IR-divergences and also to get finite values. In numerical calculation, the validity of the results must be guaranteed by comparing several independent methods. We explain shortly our consistency conditions to ensure the results. We also show some examples of calculations and how the consistency conditions are satisfied. In section 5, we give a part of our results on $(g-2)$ for restricted types of diagrams. In the last section, we summarize the present status and give some comments to make extensive progress.

2. Outline of our frame work

Our calculation is formulated under the following conditions.

- (i) Adopt non-linear gauge (NLG) formulation with 't Hooft-Feynman propagator.
- (ii) Dimensional regularization for both Ultra Violet (UV)- and Infrared (IR) -divergences.
- (iii) On mass shell renormalization scheme is adopted.
- (iv) Linear Extrapolation method (LE) is fully used for regularization and getting finite values.

Next, we briefly explain the flow of our calculation.

- (i) GRACE system generates all the diagrams we need in SM. There are 1780 two-loop diagrams and 70 one-loop diagrams composed of one-loop order counter term (CT).
- (ii) These 1780 diagrams are classified into 14 types of topology. Types of the topology are displayed in Fig.1. Among these types, some of them give the same contribution because of symmetry. (an example: 5-a vs. 5-b) The diagrams including CT are essentially two types, namely, vertex and self-energy types.

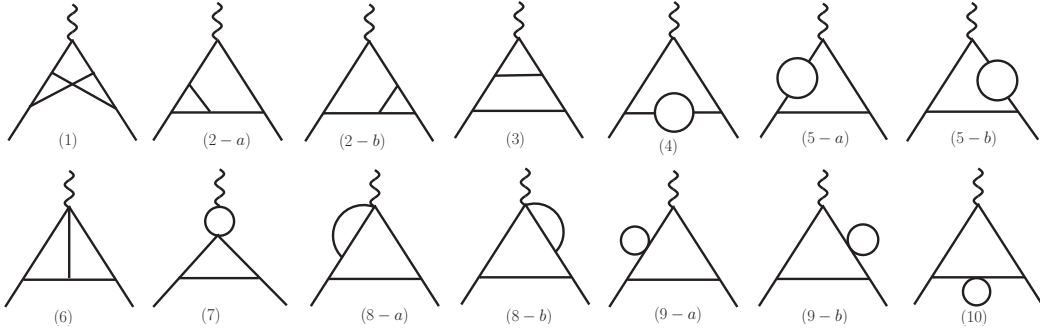


Figure 1: Types of topology

- (iii) In order to distinguish the UV-part from finite part, we prepare a few files determined by the type of topology, in advance. They represent the following quantities. [19]
 - Internal loop momentum flow $(\ell_s, \eta(s)) (s = 1, 2)$
 - External momentum flow (q_j) (j = internal line number)
 - Kirchhoff's law of momentum conservation at each vertex
- (iv) Using these tools, both UV-divergent and finite contributions to $(g-2)$ are calculated in turn, according to the formulas given in the next section [19]. We make use of a symbolic manipulation system FORM [20] exhaustively.

3. Logic of the calculation

We explain the case where there are six-propagators. Starting formula is the two-loop muon vertex,

$$\Gamma_\mu = \int \frac{d^n \ell_1}{i(2\pi)^n} \frac{d^n \ell_2}{i(2\pi)^n} \frac{F_\mu(D)}{\prod_j (p_j^2 - m_j^2)} = \Gamma(6) \int \prod dz_j \delta(1 - \sum_j z_j) \int \frac{d^n \ell_1}{i(2\pi)^n} \frac{d^n \ell_2}{i(2\pi)^n} \frac{F_\mu(D)}{\sum_j z_j (p_j^2 - m_j^2)} \quad (1)$$

where $p_j = \sum_{s=1}^2 \eta(s) \ell_s + q_j$, is the momentum on the internal line (j). The function $\eta(s) (= \pm 1, 0)$ defines loop momentum on the internal line (j). The z_j 's are the Feynman parameters to combine six propagators. The numerator function $F_\mu(D)$ is explained later.

Next we diagonalize the denominator function with respect to loop momenta ℓ_1 and ℓ_2 and perform integration. The result is,

$$\Gamma_\mu = \frac{1}{(4\pi)^n} \int \prod dz_j \delta(1 - \sum_j z_j) \frac{\Gamma(6-n)}{(\det U)^{n/2}} F_\mu(D) \frac{1}{(V - i\varepsilon)^{6-n}}, \quad U_{s,t} = \sum_{j=1}^6 z_j \eta_s(j) \eta_t(j). \quad (2)$$

Where U is well known 2×2 matrix, composed of Feynman parameters (z_j). $V(z_j, m_j, q_j)$ is the denominator function. The arguments are easily extended to the case with five-propagators (diagrams with four-point coupling).

In order to generate the numerator function we use the following differential integral operator D_μ .

$$\frac{p_j^\mu}{(p_j^2 - m_j^2)} = D_j^\mu \frac{1}{(p_j^2 - m_j^2)}, \quad \text{where} \quad D_j^\mu \equiv \frac{1}{2} \int_{m_j^2}^\infty dm_j^2 \frac{\partial}{\partial q_{j\mu}} \quad (3)$$

The operator D_j^μ generates momentum p_j^μ on the internal line (j). By operating D_j^μ to the denominator function V , we get the following expression.

$$D_j^\mu \frac{1}{V^m} = \frac{Q'_{j\mu}}{V^m}, \quad Q'_j = q_j - \frac{1}{\det U} \sum_{i=1} z_i B_{ij} q_j, \quad B_{ij} = \sum_{s,t} \eta_s(i) \eta_t(j) U_{st}^{-1} \det U = B_{ji} \quad (4)$$

Similarly we can generate the higher order term.

$$D_i^\mu D_j^\nu \frac{1}{V^m} = \frac{Q'_{i\mu} Q'_{j\nu}}{V^m} + \left(-\frac{1}{2\det U} \right) \frac{g_{\mu\nu}}{(m-1)} \frac{B_{ij}}{V^{m-1}} \quad (5)$$

We can also derive higher order terms such as $D_i^\mu D_j^\nu D_k^\lambda (1/V^m)$ and so on, however, Eq.(5) is sufficient in our case. We can verify the equivalence of the above method and the well known method of shifting momentum in the numerators. The correspondence between two methods are symbolized as follows.

$$\ell^0 \rightarrow \frac{\{1, Q'_{i\mu}, Q'_{i,\mu} Q'_{j,\nu}, \dots\}}{V^m}, \quad \ell_i \ell_j \rightarrow \left(-\frac{1}{2\det U} \right) \frac{g^{\mu\nu}}{(m-1)} \frac{B_{ij}}{V^{m-1}} \quad (6)$$

Next step is to extract the (g -2) factor by using projection operator, from the photon muon vertex Γ_μ . The quantity (g -2) is given as follows. (m_0 =muon mass)

$$\begin{aligned} (g-2) &= \lim_{q^2 \rightarrow 0} \frac{m_0}{p^4 q^2} \text{Tr}(\Gamma_\mu \text{Proj}(\mu)) \\ \text{Proj}(\mu) &= \frac{1}{4} (\not{p} - \frac{1}{2} \not{q} + m_0) \{ m_0 \gamma_\mu (p.p) - (m_0^2 + \frac{q \cdot q}{2}) p_\mu \} (\not{p} + \frac{1}{2} \not{q} + m_0), \end{aligned} \quad (7)$$

where we set momentum of incoming μ^- , outgoing μ^+ and incoming photon, as $(p-q/2)$, $(p+q/2)$ and q , respectively.

Next step is the regularization of UV-divergence. By adopting n -dimensional regularization method, any integrand F of Feynman parameter integration is regarded as a function of $\varepsilon = 4 - n/2$. Starting from the function $F(\varepsilon)$, we adopt two methods for regularization. The first method is well known one and extract $1/\varepsilon$ singularity from $F(\varepsilon)$ when one of Feynman parameters approaches 0, ($x \rightarrow 0$). Another one is called LE-method explained below [18]. We

compare two methods and conclude LE-method is simpler and more efficient than the first one if the accuracy of numerical integration is increased considerably.

First we explain the first method. In order to extract UV-divergence, we use the following procedure. First we transform the Feynman parameters (z_1, z_2, \dots, z_6) into the appropriate $[0,1]$ variables (x, y, u, v, w) depending on the topology. The key point is to factorize the function $\det U = x \times u(x, \dots)$, where $u(0, \dots) \neq 0$. Then it is shown that the UV-part in dimensional regularization comes from the following formula. We show the example of vertex type renormalization. We set $n = 4 - 2\epsilon$, $\epsilon > 0$ for UV-regularization.

$$I = \int_0^1 dx x^{\epsilon-1} F(x, \epsilon) = \frac{1}{\epsilon} F(0, 0) + \frac{\partial F(0, 0)}{\partial \epsilon} + \int_0^1 \frac{F(x, 0) - F(0, 0)}{x} dx \quad (8)$$

In the case where there is self-energy type diagram, we need the formula $\int_0^1 dx x^{\epsilon-2} F(x, \epsilon)$ in addition to Eq.(8). So it becomes more complex.

The second method named LE is applicable for both UV- and IR-regularization and obtaining finite values [18]. Space time dimension n is set to be $(4 - 2\epsilon)$ for UV-case or $(4 + 2\epsilon_R)$ for IR-case. In both cases, $\epsilon > 0, \epsilon_R > 0$.

After dimensional regularization method was introduced [21], the analyticity with respect to ϵ was discussed extensively. It is shown that the Feynman amplitude is a meromorphic function of ϵ [21] [22]. This is a key point to utilize the LE-method to the Feynman amplitude. Numerically, we calculate $G(i) = \int F(z_j, \epsilon) \prod dz_j$ when $\epsilon = \epsilon(i)$. ($i = 1, 2, \dots, M$). We set $\epsilon(i) = 1/\alpha^{i+14}$ by taking relevant value α . According to the analyticity, we can expand G and truncate it at $O(\epsilon^{M-2})$.

$$G(i) = c_{-1} \frac{1}{\epsilon(i)} + c_0 + c_1 \epsilon(i) + \dots + c_{M-2} \epsilon(i)^{M-2} = \sum_{j=-1}^{M-2} c_j \{\epsilon(i)\}^j \quad (i = 1, 2, \dots, M) \quad (9)$$

From this formula, we get $\{c_j\}$ by multiplying the inverse of $M \times M$ matrix A , whose element is $A(i, j) = \{\epsilon(i)\}^j$, ($i = 1, \dots, M$, $j = -1, 0, \dots, M-2$), to M -component vector $G(i)$. Practically we set $M \sim 15$ and $\alpha \sim 1.15$.

As for counter terms, GRACE has a library of renormalization constants at one-loop level. We make use of this library for 70-diagrams composed of counter terms. We use FORM [20] to generate Fortran source, according to the above formulation.

4. Numerical Calculation

The final step to get the value $(g-2)$ is the numerical integration over Feynman parameters. We employed trapezoidal rule with Double Exponential (DE) transformation method [23]. It is very powerful if the integrand has singular behavior at the edge of the integration domain. Speed of convergence is accelerated by the DE transformation,

$$I = \int_0^1 dx f(x) \rightarrow x = \phi(t) = \frac{1}{2} \left\{ 1 + \tanh \left(\frac{\pi}{2} \sinh(t) \right) \right\} \quad (10)$$

The maximum dimension of multiple integration is five. We apply DE-method to any integration parameter involved. As we need the accuracy of 7~10 digits to see the cancellation of UV, the adaptive Monte Carlo method is not suitable for two-loop calculation.

In order to ensure the validity of our results, we impose several conditions given below.

- (i) Well known QED two-loop value is reproduced.
- (ii) UV-divergence is cancelled.

- (iii) IR-divergence is cancelled.
- (iv) The result is independent of Non-linear gauge parameters.
- (v) In some cases (examples: topology 4,5-a,5-b,7,9-1,9b and 10) , we perform loop-integrations (ℓ_1, ℓ_2) in turn, (we call it successive method) and obtain the same results.

In all these cases, if we have plural methods to evaluate, we compare the numerical values to ascertain the validity. If all these five conditions are cleared, we can insist on the validity of our calculation.

We demonstrate how the conditions are cleared by showing the examples.

- **Reproduction of QED** two-loop value. (Unit $=(\alpha/\pi)^2$)
Analytic expression -0.328478966 : our value -0.328478911
- **UV-cancellation** in Feynman gauge (FG) among the diagrams.
Examples of a group of diagrams are shown in Fig.2.

In this case, total 13-diagrams and 1-counter term make a group to cancel UV-divergence. As you can read from the table, the cancellation is marvelous, up to almost 10 digits.

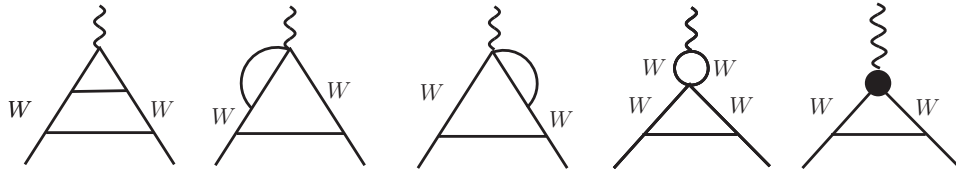


Figure 2: Sample of diagrams with W

Table 2: Sample of UV-cancellation in FG

Topology	Diagram No.	Value (unit 10^{-11})
3	149	1.679393199868
3	153	0.490572808433
3	157	0.055640154059
3	161	0.055640154059
3	171	-0.021530682050
3	172	-0.006289394980
3	173	-0.021530682050
3	174	-0.006289394980
8-a	1517	-0.166093750630
8-a	1518	-0.048518165797
8-b	1578	-0.166093750630
8-b	1579	-0.048518165797
7	1671	-2.575344486333
CT-vtx	1781	0.778962156811
	Sum	-0.0000000000017

- **IR-cancellation** is also checked by using LE-method. Among two-loop diagrams, the 8 diagrams in Fig.3 have IR-divergence. The diagrams with CT also have IR-divergence through $\delta Z_W^{1/2}$ (19-diagrams) and $\delta Z_\mu^{1/2}$ (28-diagrams). In LE-method, the IR-divergence is proportional to $C_{IR}^{(2)} = (-1/\varepsilon_R - 2\gamma + 2\ln(4\pi))$, $\varepsilon_R = (n/2 - 2)$. It is easily shown that the IR-divergence coming from $\delta Z_W^{1/2}$ cancels among the 19-CT-diagrams. As for the

diagrams with $\delta Z_\mu^{1/2}$, IR-divergence is cancelled by the corresponding two-loop diagrams. We show coefficients of $C_{IR}^{(2)}$ in Table 3. The correspondence between small photon mass (λ) method and LE-method for IR-regularization is checked in the case of QED ladder diagram. Analytic value of a coefficient of $\ln(\lambda^2/m_\mu^2)$ in unit of $(\alpha/\pi)^2$ is $(1/4)$ [5]. It is 0.249999998 by our calculation using small photon mass. In LE-method, the coefficient of $C_{IR}^{(2)}$ becomes 0.249999999 . We understand the correspondence between $\ln(\lambda^2/m_\mu^2)$ and $C_{IR}^{(2)}$ is established.

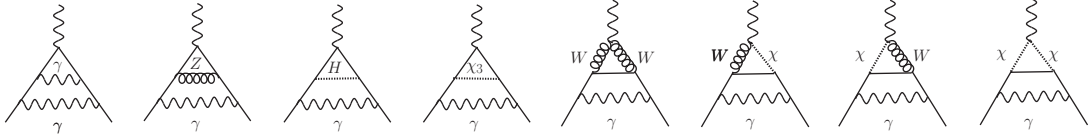


Figure 3: IR cancellation among diagrams with W and χ^\pm bosons

Table 3: Cancellation of IR-divergence (unit 10^{-11})

Diagram Type	$\delta Z_\mu^{1/2}$ Vertex CT	$\delta Z_\mu^{1/2}$ Self CT	two-loop diagram	sum
Neutral Type			diagram	
γ	-134887.2756×3	134887.2756×2	(a) $+134887.2755$	-1.6×10^{-4}
Z - boson	0.2152351626×3	-0.2152351626×2	(b) -0.2152351628	-1.7×10^{-10}
Higgs, χ_3	$1.66293755 \times 10^{-6} \times 3$	$-1.66293755 \times 10^{-6} \times 2$	$-1.66293757 \times 10^{-6}$	-2.5×10^{-14}
Charged type			diagram(c)~(h)	
W^\pm, χ^\pm	-0.4312728113299	---	0.4312728113330	3.1×10^{-12}

As we show in Table 3, no IR-divergence remains in the final expression.

- **Non-linear Gauge (NLG)** parameter independence is also checked. Non linear gauge was introduced to reduce the number of diagrams, particularly containing boson-boson couplings [24]. Here, we adopt NLG to check the validity of our calculation. The gauge fixing Lagrangian is constructed as,

$$\mathcal{L}_{GF} = -\frac{1}{\xi_W} F^+ F^- - \frac{1}{2\xi_Z} (F^Z)^2 - \frac{1}{\xi} (F^A)^2 \quad (11)$$

where

$$\begin{aligned} F^\pm &= \left(\partial^\mu \mp ie\tilde{\alpha}A^\mu \mp i\frac{ec_W}{s_W}\tilde{\beta}Z^\mu \right) W_\mu^\pm + \xi_W \left(M_W \chi^\pm + \frac{e}{2s_W}\tilde{\delta}H\chi^\pm \pm i\frac{e}{2s_W}\tilde{\kappa}\chi_3\chi^\pm \right) \\ F^Z &= \partial^\mu Z_\mu + \xi_Z \left(M_Z \chi_3 + \frac{e}{2s_W c_W}\tilde{\varepsilon}H\chi_3 \right) \\ F^A &= \partial^\mu A_\mu \end{aligned} \quad (12)$$

Here, $\tilde{\alpha}, \tilde{\beta}, \tilde{\delta}, \tilde{\varepsilon}$ and $\tilde{\kappa}$ are non-linear gauge parameters specific to this formalism. The parameters s_W and c_W are the *sine* and *cosine* of Weinberg angle θ_W . In our calculation we set $\xi = \xi_W = \xi_Z = 1$ to make the gauge boson propagators simple. As an example of cancellation of NLG parameters, we show the UV-divergent part proportional to $\tilde{\alpha}^2$. The 53 diagrams make a group and we show sum of a coefficient of $C_{UV}^{(2)} = (1/\varepsilon - 2\gamma + 2\ln(4\pi))$ for

the group of the same topological type in the Table 4. By summing up these contributions, 12 digits cancellation is confirmed even in 4 to 5 dimensional integration over Feynman parameters.

Table 4: UV-part ($\tilde{\alpha}^2$ -term)

Type	Number of diagrams	Coeff. of $C_{UV}^{(2)}$ in unit $(\alpha/\pi)^2$
2a	4	5.994906222E-08
2b	4	5.994906222E-08
3	7	-9.325381915E-06
5a	13	1.398809747E-07
5b	13	1.398809747E-07
8a	2	4.422894730E-06
8b	2	4.422894730E-06
9a	4	3.996606459E-08
9b	4	3.996606459E-08
sum(*)	53	-6.048741686E-18

(*) Each contribution is calculated in quadruple precision method and has more effective digit than shown in the table.

- **Successive method** is also applied to two-loop diagrams with self energy type two-point function. An example is diagram with $(\gamma - \gamma)$ or $(\gamma - Z)$ vacuum polarization type diagram. We decompose the renormalization constants $\delta Z_{AA}^{1/2}, \delta Z_{ZA}^{1/2}, \delta Z_{AZ}^{1/2}$ etc. into components according to the particles involved in the loop. By adding the corresponding counter term to one loop unrenormalized two-point function, we integrate over the first loop momentum ℓ_1 . The result is finite renormalized two-point function $\Pi_R(\ell_2)$. The function Π_R contains the second loop momentum ℓ_2 , however, the divergent part of ℓ_2 integration does not contribute to $(g-2)$. We use this alternative method to reconfirm the results obtained by the methods given in section 3.

5. Finite contribution from restricted type of diagrams

The publicly accepted value of ELWK two-loop correction is classified according to types of diagrams. For example, fermion loop contribution with or without Higgs boson and purely bosonic contribution are discussed separately. As an example, we summarize the naive fermion loop contribution without any approximation. The diagrams we consider are shown in Fig.4.

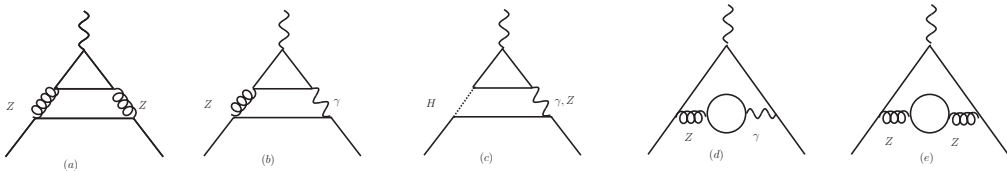


Figure 4: Fermion loop diagrams

As is shown in Fig.4, we consider diagrams with both fermion loop and neutral boson.

The contribution from fermion triangle diagrams Fig.(4-a,b) comes from VVA-anomaly. If lepton and quark mass within the same generation are degenerate, VVA-anomaly cancellation works so that the contribution becomes zero. So fermion mass difference is crucial to get the value. The $\ln(M_z^2)$ -dependence cancels within one generation, because of no-anomaly condition.

Czarnecki et al.[6] give the approximate formula for diagram Fig.(4-b). Taking the same parameters (see below), we compare their values and our exact results in Table 5.

Table 5: Comparison of Fig.(4-b) (unit 10^{-11})

lepton and quark	Ref.[6] approximate value	Our exact value
electron, up,down	-3.9984	-4.0272
muon, charm,strange	-4.6524	-4.6426
τ , top, bottom	-8.1854	-8.1940
Total	-16.8362	-16.8638

Although each fermion contribution is quite different, the coincidence becomes pretty good by taking the sum in each generation. The difference comes from the common constant terms which cancels by summing up within each generation, due to the anomaly free condition. We also show the preliminary value of other diagrams Fig.(4-a,c,d,e) in Table 6.

Table 6: Finite value Fig(4-a,c,d,e)

Type	Value	$\{10^{-11}\}$
4-a	-0.0494	
4-c	-1.8718	
4-d	-0.1803	
4-e	1.5842	

We use the following fermion and boson masses in the calculation in unit GeV. $m_\mu = 105.658389 \times 10^{-3}$, $m_e = 0.51099906 \times 10^{-3}$, $m_\tau = 1.7771$, $m_u = 0.3$, $m_c = 1.5$, $m_t = 173.21$, $m_d = 0.3$, $m_s = 0.5$, $m_b = 4.5$, $M_W = 80.22$, $M_Z = 91.187$, $M_H = 125.09$

6. Discussion and Comment

We develop the system to calculate the full ELWK two-loop corrections to $(g-2)$. Unfortunately it is not quite completely automatic system yet. We can produce Fortran source automatically. The work we need beforehand is only to prepare several files which only depend on the type of the topology of diagrams as we explained in section 2.

If we adopt the well known first method to extract UV-divergent part, it is crucial to introduce the most suitable transformations from (z_j) to $[0,1]$ integration variables (x, y, u, v, w) . In the case of Linear Expansion method (LE), however, the choice of integration variables is not sensitive to get the reliable results.

Further comments are given on the regularization method. Firstly, we introduce n -dimensional regularization method and take out UV-divergence $(1/\varepsilon)$, when one of the integration variables is approaching 0 ($x \rightarrow 0$). In order to perform this procedure, we need rather complex operations including differentiation of the amplitudes, etc. As a result, it makes Fortran source lengthy so that CPU-time increases extensively. The second prescription to regularize both UV- and IR-divergences is LE-method, briefly explained in section 3. This method decreases the number of operation drastically. It is sufficient to define the quantity as function of $\varepsilon (= 2 - n/2)$. We only need to treat Dirac matrices and various vectors appeared in the numerator, in n -dimension. This is easily done by using symbolic manipulation system such

as FORM. The operation is simple and we can make use of the resultant short sources for both UV- $(\varepsilon > 0)$ and IR- $(\varepsilon_R = -\varepsilon > 0)$ regularization and also to get finite results. By comparing the results of various methods mentioned in the previous sections, we conclude that LE-method is the most simple and reliable method, at this moment. In order to get reliable physical value by this method, accurate numerical integration over Feynman parameters is inevitable. The DE-method introduced in section 4 is the suitable candidate.

By using these technical approaches mentioned above, we clear almost all the constraints given in section 4. Namely, (i) reproduction of QED values, (ii)(iii) UV-and IR-divergences are cancelled, (iv) the result is independent of NLG-parameters. We show some samples how they are cleared. We are now recalculating and rechecking the constraints under the best computer circumstances. The final value will be given soon. We expect ongoing work provides the fruitful foundation to formulate PNQFT (Perturbative Numerical Quantum Field Theory) mentioned in section 1.2.

Acknowledgments

We would like to thank Prof.T.Kaneko for his important contribution to construct the framework of calculation at the early stage of this work. We also wish to thank Prof.K.Kato and Prof.F.Yuasa for discussion. Last but not least, we express our deep appreciation to late Prof.Y.Shimizu for his continual encouragement. This research is partially supported by Grant-in-Aid for Scientific Research (15H03668,15H03602) of JSPS.

References

- [1] Yuasa F *et al.* 2000 *Prog. Theore. Phys. Suppl.* **138** 18
- Belanger G, Boudjema F, Fujimoto J, Ishikawa T, Kaneko T, Kato K and Shimizu Y 2006 *Phys.Rept.* **430** 117
- [2] Aoyama T, Hayakawa M, Kinoshita T and Nio M 2012 *Phys.Rev.Lett.* **109** 111808
- [3] Kukhto T V, Kuraev E A, Schiller A and Silagadze Z K 1992 *Nucl.Phys.* **B371** 567
- [4] Kaneko T and Nakazawa N 1995 *Proc.of AIHENP(Artificial Intelligence for High Energy and Nuclear Physics, (Pisa,Italy)* 173
- [5] Karplus R and Kroll N M 1950 *Phys.Rev.* **77** 536
- Sommerfeld C M 1957 *Phys.Rev.* **107** 328; 1958 *Annals of Physics* **5** 26
- Petermann A 1957 *Hel.Phys.Acta* **30** 407; 1958 *Nucl. Phys.* **5** 677
- [6] Czarnecki A, Krause B and Maciano W J 1995 *Phys.Rev.* **D52** R2619
- Czarnecki A, Krause B and Marciano W J 1996 *Phys.Rev.Lett.* **76** 3267
- Czarnecki A, Marciano W J and Vainshtein A 2003 *Phys.Rev.* **D67** 073006 Erratum *ibid.* 2006 *Phys.Rev.* **D73** 119901
- [7] Gribouk T and Czarnecki A 2005 *Phys.Rev.* **D72** 053016
- [8] Marquard P 2015 *Nuclear and Particle Physics Proceedings* **260** 107
- [9] Bennett G W *et al.* 2002 *Phys.Rev.Lett.* **89** 101804
- Erratum *ibid* 2002 *Phys.Rev.Lett.* **89** 129903
- Bennett G W *et al.* 2004 *Phys.Rev.Lett.* **92** 161802
- Bennett G W *et al.* 2006 *Phys.Rev.* **D73** 072003
- [10] Patrignani C *et al.* (Particle Data Group) 2016 *Chin.Phys.* **C40** 100001 pp.715
- [11] Davier M, Hoecker A, Malaescu B and Zhang Z 2011 *Eur.Phys.J.* **C71** 1515
- [12] Prades J, de Rafael E and Vainshtein A 2009 *Advanced series on directions in high energy physics* **vol. 20** ed Roberts B L and Marciano W pp 303-317
- [13] Jackiw R and Weinberg S 1972 *Phys.Rev.* **D5** 2396
- Altarelli G, Cabibbo N and Maiani L 1972 *Phys.Lett.* **B40** 415
- Bars I and M Yoshimura 1972 *Phys.Rev.* **D6** 374
- Fujikawa K, Lee B W and Sanda A I 1972 *Phys.Rev.* **D6** 2923
- [14] Gnendiger C, Stöckinger D and Stöckinger-Kim H 2013 *Phys.Rev.* **D88** 053005
- Heinemeyer S, Stöckinger D and Weiglein S 2004 *Nucl.Phys.* **B699** 103
- [15] Mohr P J, Taylor B N and Newell D B (CODATA Group) 2012 *Rivv.Mod.Phys.* **84** 1527
- [16] Gohn W 2016 The Muon $g-2$ experiment at Fermilab *Preprint arXiv:1611.04964[hep-ex]*

- [17] Otani M (E34 collaboration) 2015 *JPS Conf.Proc.* **8** Status of the Muon g -2/EDM Experiment at J-PARC(E34) 025008
- [18] de Doncker E, Yuasa F and Kurihara Y 2011 *Proc., 3rd CPP Workshop on Computational particle physics (CPP 2010)* (Tsukuba, Japan, September 23-25,2010) p 11
de Doncker E, Fujimoto J, Hamaguchi N, Ishikawa T, Kurihara Y, Shimizu Y and Yuasa F 2012 *Journal of Computational Science* **3** 102
de Doncker E, Yuasa F, Kato K, Ishikawa T, Kapenga J and O.Olagbemi 2017, *Preprint* arXiv:1702.04904[hep-ph]
- [19] Civitanović P and Kinoshita T 1974 *Phys.Rev.* **D10** 3978, *ibid* 3991
- [20] Vermaseren J A M 2000 *preprint* arXiv:0010025[math-ph]
- [21] Bollini C G and Giambiagi J J 1972 *IL Nuovo Cimento B* **12** 20
't Hooft G and M Veltman 1972 *Nucl.Phys.* **B44** 189
- [22] Nakanishi N 1975 *Quantum Field Theory* (Tokyo:Baihukan) p.272 (in Japanese)
- [23] Takahashi H and Mori M 1974 *Publ. RIMS Kyoto Univ.* **9** 721
- [24] Boudjema Z and Chopin E 1996 *Z.Phys.Rev.* **C73** 85